

Tumorigenesis and Neoplastic Progression

Absence of Host-Secreted Protein Acidic and Rich in Cysteine (SPARC) Augments Peritoneal Ovarian Carcinomatosis

Neveen Said* and Kouros Motamed*[†]

From the Department of Pathology* and the Vascular Biology Center,[†] Medical College of Georgia, Augusta, Georgia

The matricellular glycoprotein SPARC (secreted protein acidic and rich in cysteine) possesses multifaceted roles in modulation of cell-matrix interactions, as well as tumor growth and metastasis. To investigate the influence of host-derived SPARC on peritoneal dissemination of ovarian cancer, we established a murine model that faithfully recapitulates advanced human disease by intraperitoneal injection of syngeneic ID8 ovarian cancer cells into SPARC-null and wild-type mice. Compared to wild-type mice, SPARC-null mice showed significantly shorter survival and developed extensive nodular peritoneal dissemination with hemorrhagic ascitic fluid accumulation. Ascitic fluid collected from SPARC-null mice showed significantly augmented levels and activity of vascular endothelial growth factor and gelatinases. Immunohistochemical analysis of tumor nodules from SPARC-null mice revealed higher proliferation and lower apoptosis indices with minimal staining for major extracellular matrix constituents. *In vitro*, SPARC significantly suppressed adhesion to and invasion of various peritoneal extracellular matrix constituents by murine and human ovarian cancer cell lines. Our findings suggest that SPARC ameliorates ovarian peritoneal carcinomatosis through abrogation of the initial steps of disease pathogenesis, namely tumor cell adhesion and invasion, inhibition of tumor cell proliferation, and induction of apoptosis. Thus, SPARC represents an important therapeutic candidate in ovarian cancer. (Am J Pathol 2005, 167:1739–1752)

Ovarian cancer ranks fourth in cancer deaths among women, accounting for more deaths than any other cancer of the female reproductive system with an estimated 22,220 newly diagnosed cases and 16,210 deaths in 2005¹ (<http://www.cancer.org>). Preferential involvement

of the peritoneal structures occurs after direct spread of malignant cells from the primary tumor to the peritoneal cavity followed by a cascade of events of which adhesion of tumor cells to the peritoneal surface is the key step. Ovarian cancer cells have the ability to bind to extracellular matrix (ECM) constituents that are either produced by peritoneal mesothelial cells or become exposed as a result of peritoneal involvement secondary to tumor cell invasion.² Adhesion is followed by a cascade of consecutive but somewhat overlapping cycles of tumor cell proliferation, migration on the peritoneal surface, cell shedding from the primary growth, readhesion to different peritoneal sites and at later stages, invasion of extraperitoneal structures. Concomitant with the aforementioned steps, overproduction of vascular endothelial growth factor (VEGF) by tumor cells results in increased permeability of the peritoneal blood vessels with subsequent exudation and accumulation of ascitic fluid, which in turn supports the growth and proliferation of floating tumor cell aggregates.^{3–5}

SPARC (secreted protein acidic and rich in cysteine) is an ECM-associated 32-kd glycoprotein that mediates cell-matrix interactions, but does not serve a primary structural role. Besides its well-documented counteradhesive and anti-proliferative functions, SPARC is implicated in regulation of the ECM production, assembly, and degradation, as well as modulation of angiogenesis. These functions have mainly been attributed to the ability of SPARC to bind ECM proteins and to modulate the effects of growth factors on stromal cells.^{6,7} The involvement of SPARC in different tumors is reported to be contextual due to the diverse functions of SPARC in a given microenvironment.^{8,9} Whereas the expression of

Supported in part by the Georgia Cancer Coalition (grant GCC0023 to K.M.) and the National Institutes of Health (grant K01-CA089689 to K.M.).

Accepted for publication August 4, 2005.

Supplemental material for this article can be found on <http://ajp.amjpathol.org>.

Address reprint requests to Kouros Motamed, Ph.D., Medical College of Georgia, Vascular Biology Center and Department of Pathology, 1459 Laney Walker Blvd., CB3306, Augusta, GA, 30912. E-mail: kmotamed@mcg.edu.

SPARC has been identified as a marker of invasiveness in certain cancers,^{10,11} suppression of SPARC expression was positively correlated with the invasiveness and the late stages of human ovarian cancer.^{12,13} It has been shown that SPARC is down-regulated in ovarian carcinoma cells and that restoring SPARC expression in stable-transfectants of ovarian cancer cells leads to reduced growth and tumorigenicity.¹⁴ Furthermore, SPARC was found to induce apoptosis in human ovarian carcinoma cells *in vitro*.¹⁵ Thus, SPARC appears to control malignancy in the ovarian epithelium but the exact underlying molecular pathways have not yet been fully elucidated.

SPARC-null ($SP^{-/-}$) mice are fertile and immunocompetent. They are characterized by decreased type I collagen fibrillogenesis that is believed to play a major role in regulating the response of these animals to dermal wounding, implanted foreign bodies and tumor cells, as well as development of osteopenia.¹⁶⁻¹⁹ They are also characterized by early-onset cataractogenesis.²⁰⁻²²

Herein, we report, for the first time, the generation of a syngeneic mouse model of ovarian cancer in $SP^{-/-}$ mice that not only recapitulates the advanced stages of human disease but also provides an important tool to study the influence of SPARC on the biology of ovarian carcinoma in an otherwise immunocompetent host. This model is also valuable for the investigation of the molecular interactions of host versus tumor SPARC and the multifaceted effects of SPARC on tumor microenvironment homeostasis.

Materials and Methods

Cell Culture and Reagents

ID8, a cell line that was derived from spontaneous *in vitro* malignant transformation of C57BL/6 mouse ovarian surface epithelial cells,²³ and was stably transfected with a retroviral vector expressing green fluorescent protein, was a generous gift from Dr. George Coukos (University of Pennsylvania, Philadelphia, PA). ID8 cells were maintained in Dulbecco's modified Eagle's medium (DMEM), supplemented with 2 mmol/L L-glutamine (Sigma, St. Louis, MO). Human ovarian cancer cell lines SKOV3 and NIH:OVCAR3 were purchased from American Type Culture Collection (Rockville, MD), and were maintained in McCoy's medium (Sigma) and RPMI 1640 (American Type Culture Collection) supplemented with 5 μ g/ml bovine insulin (Sigma), respectively. All media were supplemented with 5 to 15% fetal bovine serum (Atlanta Biologicals, Norcross, GA) and 100 U/ml penicillin and 100 μ g/ml streptomycin (Sigma). SPARC from mouse parietal yolk sac was purchased from Sigma. The levels of endotoxin in SPARC were found to be less than 0.1 EU/mg, as determined by Limulus amoebocyte lysate (LAL; Associates of Cape Cod, Woods Hole, MA). Collagen I (Col I) from rat tail, mouse collagen IV (Col IV), and mouse EHS laminin (LN) were purchased from BD Biosciences (Bedford, MA). Human plasma fibronectin (FN), human plasma vitronectin (VN), and human umbilical vein hyal-

uronic acid (HA) were purchased from Sigma. All other chemicals were analytical grade and were purchased from Sigma or Fisher Scientific (Fairlawn, NJ).

Mice

C57BL/6 \times 129SvJ SPARC-null ($SP^{-/-}$) and wild-type ($SP^{+/+}$) mice (6 to 8 weeks old) were used in the tumor studies and were a kind gift of Dr. Helene Sage (Hope Heart Program, Benaroya Research Institute at Virginia Mason, Seattle, WA). Mice were backcrossed against wild-type C57BL/6 mice for at least six generations before use in tumor studies. All experimental procedures were approved by the Laboratory Animal Services of the Medical College of Georgia and were performed in specific pathogen-free facilities.

In Vivo Tumor Generation

Subconfluent ID8 cells were harvested by trypsinization and washed three times in Dulbecco's phosphate-buffered saline by centrifugation at $2000 \times g$ for 3 minutes. A single cell suspension was prepared in Dulbecco's phosphate-buffered saline and the concentration was adjusted to 7×10^7 cells/ml.²⁴ For intraperitoneal tumor generation, $SP^{+/+}$ and $SP^{-/-}$ mice ($n = 10$ per group) were anesthetized with isoflurane and 0.7 ml ($\sim 5 \times 10^7$ cells) of the ID8 cell suspension was inoculated in the peritoneal cavity via a 27-gauge sterile syringe (Fisher Scientific). Animals were monitored twice weekly for tumor development and survival (up to 10 weeks). Tumor growth was determined by weekly measurements of animal girth and weight. At the end of the experimental period (7 weeks), animals were sacrificed and organs were examined for tumor development and spread. Ascitic fluid from the animals that developed peritoneal tumors was collected, centrifuged at $1000 \times g$ and the supernatants were collected and stored at -80°C for further processing.

Live Fluorescent Stereomicroscopy

The gross morphology of tumor growth and the extent of dissemination in the peritoneal cavity were observed and documented using a fluorescent stereomicroscope equipped with Q-Imaging digital camera (Leica Microsystems, Wetzlar, Germany). Tumor dissemination in the peritoneal cavity was scored on two arbitrary scales based on the number and size of tumor nodules under dissecting microscope equipped with epifluorescent illumination (Leica Microsystems). Based on tumor nodule size, each animal was given an arbitrary score from 0 to +4: 0, for tumor-free animals with undetectable nodular growths; +1, for nodules <1 mm in diameter or those only visualized by fluorescent stereomicroscopy; +2, for nodules 1 to 5 mm in diameter, +3, for nodules 5 to 10 mm; and +4, for nodules >10 mm. Based on the number of nodules in the peritoneal surface and abdominal structures, another scale from 0 to +4 was set: 0, for tumor-free; +1, for 0 to 5 nodules/examined organ, including nodules that were only detected by fluorescent stereomi-

croscope; +2, for 5 to 10 nodules/organ; +3, for 10 to 15 nodules; +4, for >20 nodules including nodular plaques and omental caking. Results were expressed as the mean score \pm SEM for each animal.

Histology and Immunohistochemical Analysis

Segments of the peritoneum showing tumor growth as well as subcutaneous tumors were processed as follows: one third was frozen, one third was fixed in methyl Carnoy's fixative, and one third was fixed in 10% neutral-buffered formalin (Fisher Scientific). Methyl Carnoy's and formalin-fixed tissues were embedded in paraffin and were cut in 5- μ m sections. Formalin-fixed tissues were stained with hematoxylin and eosin (H&E) (Fisher Scientific), Masson's trichrome (Sigma), and Picrosirius red (Sigma) according to standard protocols.^{10,19} Methyl Carnoy's-fixed and formalin-fixed tissues were deparaffinized and blocked with 0.3% H₂O₂ in methanol. Some of the sections were subsequently treated with AutoZyme (10- μ l enzyme concentrate/ml buffer for 15 to 30 minutes at room temperature; BioMeda Corp., Foster City, CA). Antibodies requiring AutoZyme treatment were rat anti-LN α 1, rabbit anti-mouse Col I, rabbit anti-Col IV, rat anti-FN, rabbit anti-mouse VEGFR1, rabbit anti-mouse VEGFR2 (Chemicon, Temecula, CA), and goat anti-mouse VEGF (R&D Systems, Minneapolis, MN). The antibodies that did not require antigen retrieval were rat anti-mouse CD31 (BD Pharmingen, San Diego, CA), rat anti-mouse MECA32 (Developmental Studies, Hybridoma Bank, University of Iowa, Iowa City, IA), rat anti-Ki67 (BD Pharmingen), and rabbit anti-phospho-histone H3 (Upstate Biotechnology Inc., Lake Placid, NY). Sections were incubated with the primary antibodies for 2 hours at room temperature, washed with phosphate-buffered saline (PBS)-0.2% Tween-20 (PBST) and incubated for 1 hour with peroxidase-labeled appropriate secondary antibody (Jackson ImmunoResearch Laboratories Inc., West Grove, PA). Sections were developed with Vectastain ABC Elite kit (Vector Laboratories, Burlingame, CA) and stable 3,3'-diaminobenzidine (ResGen, Huntsville, AL), counterstained with hematoxylin, and mounted in permount (Fisher Scientific). Images were acquired with a Leica microscope (DM5000) equipped with a Q-Imaging digital camera.

VEGF Enzyme-Linked Immunosorbent Assay (ELISA)

A Quantikine mouse VEGF ELISA kit (R&D Systems) was used to determine VEGF levels in the collected ID8 culture supernatants, as well as in the ascitic fluid samples according to the manufacturer's instructions. Briefly, samples were diluted 1:1, 1:5, and 1:100 in the sample diluent provided in the kit and incubated in wells of 96-well plates precoated with polyclonal anti-VEGF antibody for 2 hours at room temperature. After washing and blocking nonspecific reactions, wells were incubated with peroxidase-labeled monoclonal anti-VEGF antibody for another 2 hours at room temperature. The reaction

was then developed with the 3-ethylbenzthiazoline-6-sulfonic acid (ABTS) system and the absorbance was read at 405 nm (A₄₀₅). VEGF concentrations in test samples were determined by comparison with a standard curve generated with known concentrations of mouse VEGF₁₆₄.

Adhesion Assays

Wells of 24-well tissue culture plates were coated with FN (50 μ g/ml), Col I (50 μ g/ml), LN (50 μ g/ml), Col IV (50 μ g/ml), VN (1 μ g/ml), and HA (1 mg/ml) in PBS overnight in a humidified incubator at 37°C. Wells were blocked with 2% bovine serum albumin (BSA) in PBS for 1 hour and then gently washed with PBS. ID8 cells were harvested in 0.5% trypsin/2 mmol/L ethylenediamine tetraacetic acid (EDTA), resuspended in DMEM/0.5% BSA at 1×10^6 cells/ml and 300 μ l was added to each well. Plates were incubated for 5 hours in a humidified incubator at 37°C, 5% CO₂. Wells were washed three times in PBS to remove nonadherent cells and were then stained with Hemacolor 3 stain (Fisher Scientific), as recommended by the manufacturer. The number of adherent cells in three fields per well were quantified using an inverted microscope equipped with DFC 320 digital camera (Leica) under 200 \times magnification. Studies were done in triplicates per experimental condition. To determine the inhibitory effect of SPARC on the adhesion of murine and human ovarian cancer cell lines to different matrices, the assays were performed in the presence of 40 μ g/ml of SPARC for 5 hours. Controls included cells incubated with the vehicle (PBS containing Ca²⁺ and Mg²⁺, Sigma) as well as cells incubated in uncoated wells and wells coated with 2% BSA. Because FN was determined to be the most favorable ECM protein for adhesion, it was used to determine whether ascitic fluid from tumor-bearing SP^{+/+} and SP^{-/-} mice influence the adhesion of ID8 cells. Pooled ascitic fluid samples (with equivalent protein concentrations) from SP^{-/-} and SP^{+/+} mice were serially diluted in DMEM and were incubated with ID8 cells in FN-coated wells for 5 hours. All experiments were done in triplicates per experimental condition and the results were expressed as the mean \pm SEM.

Invasion Assays

Confluent ID8, OVCAR3, and SKOV3 monolayers were starved overnight in serum-free DMEM. Cells were harvested in PBS-0.5% EDTA and collected by centrifugation. A suspension of cells (2×10^5 cells in appropriate growth medium containing 0.5% BSA) in the presence or absence of 40 μ g/ml of SPARC was added to the upper chamber of polycarbonate inserts (8- μ m pore size, 6.5 mm diameter, and 10 μ m thickness; Corning Costar, Corning, NY). Inserts were precoated with either FN (50 μ g/ml), Col I (50 μ g/ml), Col IV (50 μ g/ml), LN (50 μ g/ml), VN (1 μ g/ml), or HA (1 mg/ml). The inserts were placed in 24-well culture plates (Corning Costar) containing appropriate complete growth medium. After a 5-hour incubation at 37°C/5% CO₂, cells in the top chamber were

removed by Q-tips (Fisher Scientific) and cells attached to the underside of the inserts (the invasive cells) were stained with Hemacolor 3 stain. Cells were counted in four fields per insert with an inverted microscope equipped with DFC 320 digital camera (Leica) under 200 × magnification. In our pilot studies, the doubling times of ID8, SKOV3, and OVCAR3 cells in culture were calculated to be 18, 20, and 40 hours, respectively (data not shown). Hence, it was safely assumed that proliferation was not a contributing factor in this type of assay. To determine whether ascitic fluid from tumor-bearing mice influences the invasion of FN by ID8 cells, pooled ascitic fluid samples from *SP*^{-/-} and *SP*^{+/+} mice were serially diluted in DMEM and were incubated with ID8 cells in FN-coated wells for 5 hours. All experiments were done in triplicates and the results were expressed as the mean ± SEM.

Proliferation Assays

Nonradioactive Cell Proliferation Assay

CellTiter⁹⁶ kit (Promega, Madison, WI) was used to assess the effect of SPARC or ascitic fluid at the indicated concentrations for 48 hours, 1 day after seeding ID8 cells into 96-well plates. The number of proliferating cells was determined colorimetrically by measuring the absorbance at 590 nm (A_{590}) of the dissolved formazan product after the addition of MTS for 3 hours, as described by the manufacturer. Proliferation index was determined as the ratio of the number of viable cells with the indicated treatment to control cells without treatment. All experiments were performed in triplicates and the results were expressed as the mean ± SEM.

Bromodeoxyuridine (BrdU) ELISA

BrdU incorporation was measured to determine DNA synthesis by proliferating cells. The Cell Proliferation Bio-trak ELISA kit (Amersham Biosciences Corp., Piscataway, NJ) was used according to the manufacturer's instructions. Briefly, 5000 cells in 100 μl of complete medium were seeded onto 96-well plates in triplicates and allowed to attach overnight. Cells were incubated with the indicated concentrations of the test materials for 48 hours and were labeled with 100 μmol/L BrdU in serum-free medium for 3 hours at 37°C/5% CO₂ in a humidified incubator. After removal of the labeling medium, cells were fixed and incubated in blocking buffer for 30 minutes to block nonspecific binding. Anti-BrdU antibody was then added to the cells for 90 minutes at room temperature, followed by extensive washing in the provided wash buffer. The reaction was developed with TMB substrate for 15 minutes, stopped with 1 mol/L sulfuric acid, and absorbance was read at 450 nm (A_{450}) within 5 minutes. All experimental conditions were performed in triplicates and the results were expressed as the mean ± SEM.

In Situ Terminal dUTP Nick-End Labeling (TUNEL) Assay

A colorimetric TUNEL *in situ* detection kit (Promega) was used to detect apoptotic cells *in vitro* and *in vivo*. The procedure was performed according to the manufacturer's instructions. Briefly, tumor sections were deparaffinized in xylene and descending grades of ethanol, and were subsequently digested with the provided proteinase K followed by a 5-minute paraformaldehyde (Fisher Scientific) fixation. Cells grown on slide chambers were fixed for 15 minutes in 4% paraformaldehyde in PBS followed by permeabilization in 0.1% Triton X-100 in PBS for 5 minutes. After incubation of either tumor sections or cells with residues of digoxigenin-labeled nucleotides and terminal nucleotide transferase for 1 hour at 37°C, they were incubated with peroxidase-labeled anti-digoxigenin antibody for 1 hour at room temperature. DNA fragments were then visualized with 3,3'-diaminobenzidine and H₂O₂. Controls included cells or sections treated with DNase I (Ambion Inc., Austin, TX) and without incubation with the digoxigenin-labeled nucleotides and terminal nucleotide transferase as positive and negative controls, respectively.

RNA Isolation and Reverse Transcriptase-Polymerase Chain Reaction

RNA was isolated from tissues with Trizol reagent (Invitrogen, Carlsbad, CA). After treatment with RNase-free DNase (Ambion Inc.) for 15 minutes at room temperature, RNA was further purified with RNeasy isolation kit (Qiagen, Valencia, CA). Total RNA (2 μg) was reverse-transcribed in 20 μl of reaction system using Improm II RT enzyme kit (Promega) as described by the supplier. Reverse-transcribed cDNA was amplified in a 20-μl reaction system containing 200 μmol/L each dNTP (Promega), 25 pmol of each primer, with the standard buffer containing 1U Jumpstart *Taq* polymerase (Sigma) and 1.5 mmol/L MgCl₂. After initial denaturation at 94°C for 4 minutes, polymerase chain reaction was performed at 94°C for 30 seconds, 56°C for 45 seconds, and 72°C for 1 minute. The final extension was at 72°C for 8 minutes. Specific oligonucleotide primers were designed according to published sequences (Table 1). Polymerase chain reaction products were resolved in 1.8% agarose gel and were visualized with ethidium bromide staining under UV light. Gel imaging, documentation, and analysis were done with a Kodak Logic Gel 100 imaging system equipped with Kodak D 3.6 software (Eastman-Kodak, Rochester, NY).

Gelatin Zymography

Gelatin zymography was performed according to published protocols.²⁵ Briefly, ascitic fluid samples (30 μg protein, as determined by BCA microassay kit; Pierce, Rockford, IL) were denatured in the absence of reducing agent and electrophoresed in 8% sodium dodecyl sulfate-polyacrylamide gel electrophoresis containing 0.1% (w/v) gelatin (Sigma). Gels were subsequently washed twice for 1 hour at

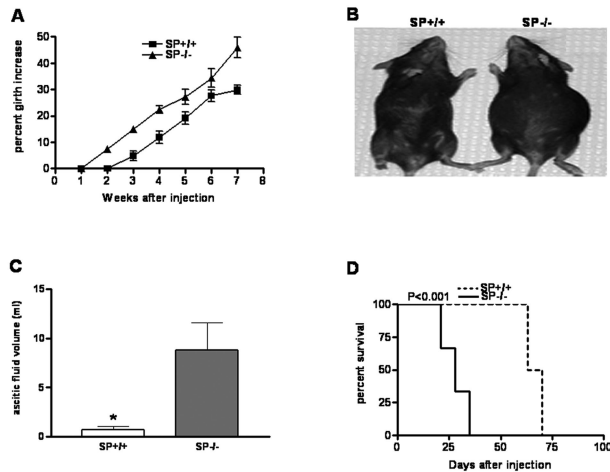


Figure 1. Accelerated intraperitoneal ID8 ovarian carcinoma growth and ascites formation in SPARC-null mice. **A** and **B**: Relative to $SP^{+/+}$ controls, $SP^{-/-}$ mice showed both an accelerated and a pronounced increase in girth at all time points studied ($P < 0.05$ at each time point, $n = 10/\text{group}$). **C**: $SP^{-/-}$ mice accumulated significantly larger volumes of hemorrhagic ascitic fluid than $SP^{+/+}$ counterparts ($*P < 0.01$, $n = 10/\text{group}$). **D**: Intraperitoneal injection of ID8 cells resulted in significantly reduced median survival in $SP^{-/-}$ mice, relative to their $SP^{+/+}$ counterparts ($*P < 0.001$, $n = 10/\text{group}$). Results shown are from one experiment that was representative of at least two independent studies.

room temperature in 2.5% Triton X-100 (Sigma), followed by incubation at 37°C overnight in a buffer consisting of 10 mmol/L CaCl_2 , 0.15 mol/L NaCl, and 50 mmol/L Tris-HCl (pH 7.5). Gels were stained for protein with 0.25% Coomassie blue (Fisher Scientific). Proteolysis was detected as a white zone in a blue background and photographed using a Kodak Gel Logic 100 imaging system equipped with Kodak D 3.6 software.

Statistical Analysis

Statistical analysis was done using GraphPad Prism version 3.1 for Windows (GraphPad Software, San Diego CA). Survival curves were generated using the Kaplan-Meier method followed by log-rank test for comparison of curves. The changes in the girth measurements as a function of time, as well as the concentration-dependent studies were performed by one-way analysis of variance followed by Newman-Keuls multiple comparison test. Comparison of tumor nodule scores was performed by Mann-Whitney test. All other statistical analyses were determined by Student's *t*-test. Differences were considered significant at $P < 0.05$.

Results

Absence of Host-Derived SPARC Dramatically Accelerates Ascites Formation and Peritoneal Metastasis in Vivo

After intraperitoneal implantation of ID8 cells, 9 of 10 $SP^{-/-}$ animals developed peritoneal tumors, compared to only 4 of 10 $SP^{+/+}$ counterparts. $SP^{-/-}$ mice exhibited faster rates of tumor development and ascitic fluid accumulation (manifested in the live animal by a significant increase in girth), relative to $SP^{+/+}$ controls. At all experimental time points, the percentage of girth increase was significantly higher in $SP^{-/-}$, compared to their $SP^{+/+}$ counterparts ($45.9\% \pm 3.9$ and $29.9\% \pm 1.8$, respectively; Figure 1, A and B). $SP^{-/-}$ mice also accumulated larger volumes of hemorrhagic ascitic fluid than controls (8.8 ± 2.7 ml and 0.7 ± 0.3

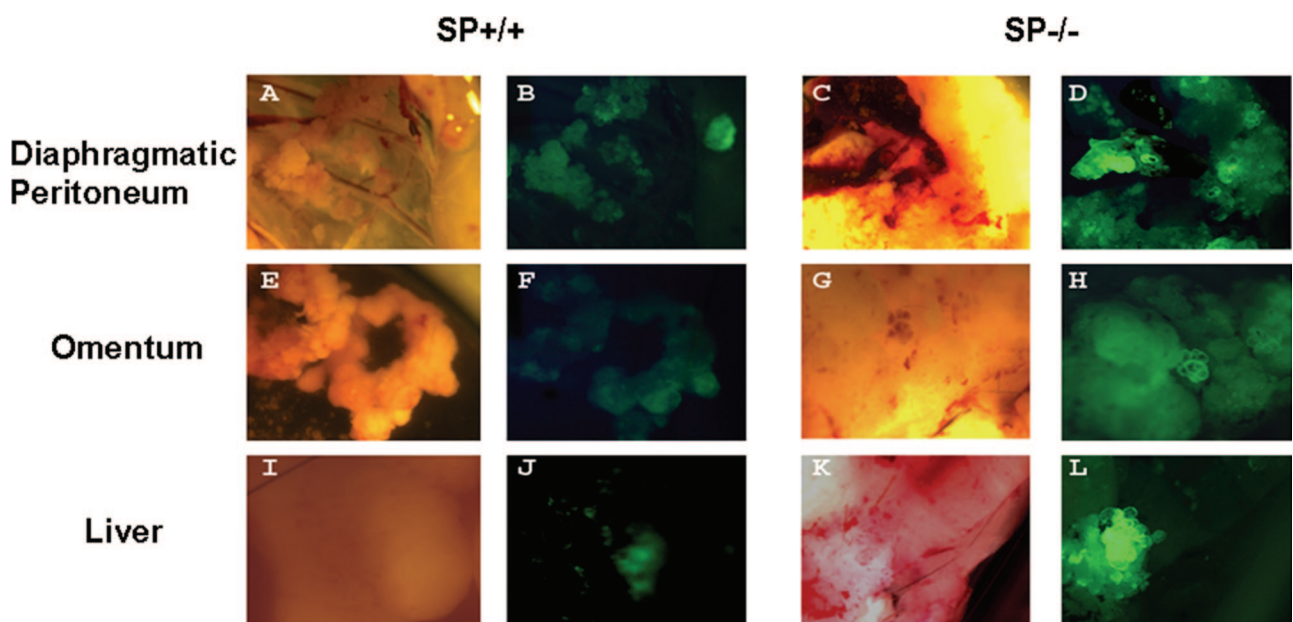


Figure 2. Bright-field (**A, C, E, G, I, K**) and fluorescent (**B, D, F, H, J, L**) stereomicroscopy of peritoneal carcinomatosis. Fluorescent tumor nodules were mainly detected under the diaphragm with localized nodular tumors in $SP^{+/+}$ (**A, B**), compared to the extensively diffuse nodules in $SP^{-/-}$ mice (**C, D**). Involvement of the omentum and the intestinal loops were much reduced in $SP^{+/+}$ (**E, F**), relative to $SP^{-/-}$ controls (**G, H**). Nodules in porta hepatis and adjacent liver lobules were less pronounced in $SP^{+/+}$ (**I, J**) than the larger nodules in $SP^{-/-}$ counterparts (**K, L**).

Table 1. PCR Primers Used in Semiquantitative RT-PCR

Primer name		Primer sequence	Cycle no.
rpS6	F	5'-AAGCTCCGCACCTTCTATGAGA-3'	24
	R	5'-TGACTGGACTCAGACTTAGAAGTAGAAGC-3'	
VEGF	F	5'-AGGCTGTGATAAGGATGAAGC-3'	30
	R	5'-CCGCCTTGCTTGTAC-3'	
VEGFR 1	F	5'-GTCTGCTTAGGTCGTGCACAC-3'	35
	R	5'-CTGGATGAGAACTCAGGCT-3'	
VEGFR 2	F	5'-CGAGTCTGTCTACCTTGGAGGC-3'	35
	R	5'-CAGCCTGAGCCTTTACCGC-3'	
Npn 1	F	5'-ACCACTGATAACTCGATTTGTCCG-3'	30
	R	5'-CGATCTTGAACCTCCTGAACAC-3'	
MMP-2	F	5'-TTGGATATTTGCAATGCAGCC-3'	35
	R	5'-AAGTTGAGGAACGAGCGA-3'	
MMP-9	F	5'-CCATTTTCGACGACGAGT-3'	35
	R	5'-CCAAATTTGCCGTCTTATCGTA-3'	

ml, respectively; Figure 1C). Moreover, the significantly augmented tumor growth in *SP*^{-/-} mice culminated in much reduced median survival rates, relative to *SP*^{+/+} controls (6 and 10 weeks, respectively; Figure 1D). Live fluorescent stereomicroscopy of the sacrificed animals at the end of 6 weeks revealed significantly more diffuse peritoneal carcinomatosis in *SP*^{-/-} mice, consisting of multiple tumor nodules up to 15 mm in diameter throughout the parietal and visceral surfaces of the peritoneum (Figure 2 and Table 2). Tumor nodules were more pronounced in the diaphragmatic surface of the peritoneum and formed nodular plaques (Figure 2, A to D). In the omentum, tumor growth caused marked adhesions of the intestinal loops and extended to the pelvic peritoneum, whereas *SP*^{+/+} mice developed significantly fewer and smaller tumor nodules (~1 to 3 mm in diameter; Figure 2, E to H). Metastases in the liver (Figure 2; I to L), peritoneal attachment of the hilum of the spleen, ovary, and lung were mostly detected in *SP*^{-/-} animals but were minimal or nonexistent in *SP*^{+/+} counterparts (data not shown).

Tumor Growth in *SP*^{-/-} Mice Is Associated with Alteration in the ECM

Recent studies have reported defective accumulation of the ECM in tumors implanted subcutaneously in *SP*^{-/-} mice, as compared to *SP*^{+/+} controls.^{10,19,27} We hypothesized that the lack of host-derived SPARC might also influence intraperitoneal ID8 tumor growth

by alteration of the ECM within and around the tumor mass. First, we examined the nontumor-bearing peritoneal sections from *SP*^{+/+} and *SP*^{-/-} animals. We found that *SP*^{+/+} had a more defined mesothelial layer than *SP*^{-/-} counterparts (Figure 3A, top). Masson's trichrome staining (Figure 3A, middle) revealed that Col I and Col III levels were significantly augmented in the mesothelial layer in *SP*^{+/+} peritoneal sections, relative to that in *SP*^{-/-} counterparts. Picrosirius red staining (Figure 3A, bottom) revealed the immaturity of Col I fibrils (yellow-green birefringence under polarized light) in *SP*^{-/-} animals, compared to mature fibrils (red birefringence under polarized light) in *SP*^{+/+} controls. Diminution of Col I in the mesothelial layer of *SP*^{-/-} peritoneal sections was further confirmed by immunostaining (data not shown). However, no significant alterations in the levels of other ECM constituents were detected (data not shown). In tumor-bearing *SP*^{-/-} animals, H&E staining revealed extensive nodular tumors composed of multiple layers of malignant cells that invaded the deeper mesothelial and submesothelial layers, reaching the adjacent muscular layer of the diaphragm and the muscles of the anterior abdominal wall (Figure 3B). Smaller tumor nodules with fewer layers of cells and well-defined mesothelial and submesothelial layers were also detected adjacent to the large nodules and represented recent seedlings of the tumor cells onto the peritoneal surface. In *SP*^{+/+} animals, nodules were significantly smaller than *SP*^{-/-} animals and comprised fewer layers of malignant cells overlying well-defined mesothelial and submesothelial layers. Masson's trichrome staining revealed significantly increased collagen staining within and underneath tumor nodules in *SP*^{+/+} mice, relative to *SP*^{-/-} mice. Picrosirius red staining revealed that the birefringence of collagen fibers was localized in the mesothelial and submesothelial layers in *SP*^{+/+} tumors, but was markedly attenuated in that of *SP*^{-/-} tumors. Immunostaining of peritoneal tumors (Figure 4) showed more ECM (Col I, Col IV, LN, and FN) staining within and around the tumor cells in the nodules of *SP*^{+/+} tumors, whereas in *SP*^{-/-} tumors, only nodular growths in the immediate vicinity of the mesothelial

Table 2. Summary of the Average Score of Peritoneal Tumor Nodules

	<i>SP</i> ^{+/+}	<i>SP</i> ^{-/-}
Diaphragm	1.2 ± 0.35	3.65 ± 0.11
Omentum	0.95 ± 0.31	3.7 ± 0.11
Peritoneal wall	0.75 ± 0.24	3.35 ± 0.15
Liver (porta hepatic and adjacent lobes)	0.7 ± 0.25	2.6 ± 0.15
Stomach (curvatures)	0.25 ± 0.1	2.3 ± 0.11
Spleen (hilum)	0.3 ± 0.13	2.2 ± 0.2
Kidney surface	0.3 ± 0.15	2.6 ± 0.17
Pancreatic surface	0.75 ± 0.24	2.45 ± 0.15
Pelvis	0.65 ± 0.2	2.5 ± 0.11

surface exhibited Col I, Col IV, and FN staining within and around the tumor cells with minimal LN staining.

SPARC Inhibits the Adhesion of ID8 Cells to ECM Constituents

It is known that intraperitoneal dissemination of tumor cells requires the adhesion of malignant cells to various collagenous and noncollagenous major constituents of the ECM (FN, VN, HA, and Col I) and the basement membrane (LN, Col IV) on the peritoneal surface.^{3,4,28} The counteradhesive property of SPARC has been documented in endothelial cells.^{29,30} We hypothesized that the decrease in tumor size in *SP*^{+/+} mice may be due to the counteradhesive effect of SPARC on the adhesion of ovarian cancer cells to ECM components. We found that ID8 cells significantly adhered to all of the aforementioned ECM constituents (*P* < 0.001, compared to BSA control) with maximum adhesion to Col IV, followed by VN, FN, Col I, HA, and LN. The adhesion of ID8 cells to these matrix molecules was partially, yet significantly (48 to 73%), inhibited by SPARC (Figure 5A). Consistent with these findings, SPARC was shown to exert a significant counteradhesive effect (35 to 75%) on both the highly

metastatic (SKOV3) and the less metastatic (OVCAR3) human ovarian cancer cell lines (Figure 5, B and C).

SPARC Inhibits the Invasion of ECM by ID8 Cells

Intraperitoneal dissemination is characteristic of ovarian carcinomas and the interstitial matrix constitutes the active sites of invasion, such as serosa of the bowels and the submesothelial connective tissue of the peritoneum. Adhesion of the disseminating tumor cells to the interstitial matrix is a prerequisite for their subsequent invasion.³¹ Since we were able to show that SPARC partially inhibits the adhesion of murine and human ovarian carcinoma cells to the ECM constituents, we sought to determine whether it would also suppress their invasiveness. Results of our invasion experiments revealed that ID8 cells and OVCAR3 cells were able to invade FN, Col IV, and VN more efficiently than Col I, LN, or HA. Moreover SKOV3 cells displayed more efficient invasion of FN, Col IV, Col I, and VN than that of HA and LN. SPARC significantly inhibited invasion of various matrices by ID8 cells (64 to 83%, Figure 6A), OVCAR3 (24 to 75%, Figure 6B), and SKOV3 (51 to 75%, Figure 6C).

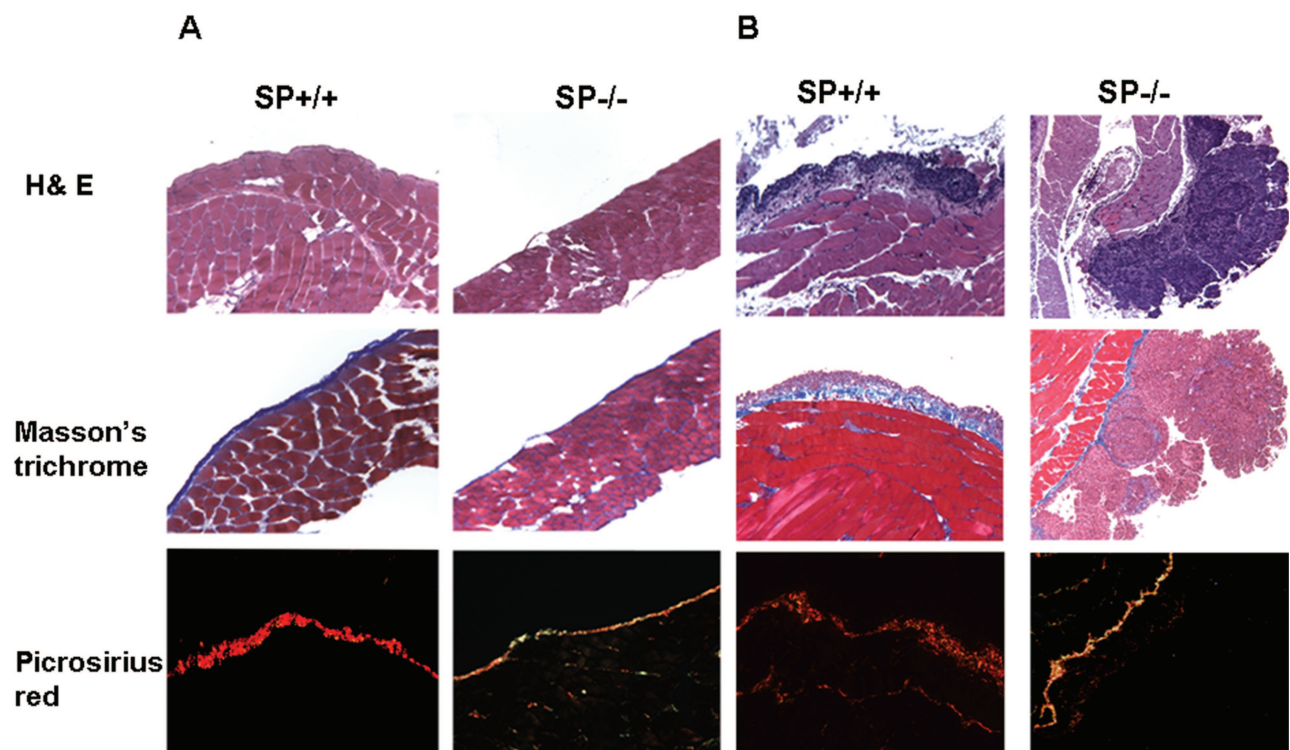


Figure 3. Enhanced peritoneal tumor growth in *SP*^{-/-} mice is associated with alteration of the level and maturity of collagen. H&E staining of normal (nontumor bearing) peritoneal sections revealed reduced thickness of the mesothelial layer in *SP*^{-/-} sections, compared to *SP*^{+/+} counterparts (**A, top**). *SP*^{-/-} peritoneal sections also displayed a less abundant collagen layer (blue) with Masson's trichrome staining (**A, middle**) and immature collagen fibrils (yellow-green birefringence under polarized light) with Picosirius red stain (**A, bottom**). H&E staining of sections from peritoneal tumors revealed smaller nodules with fewer cell layers overlying a wider submesothelial layer in *SP*^{+/+} tumor, compared to larger nodules with multiple cell layers overlying a poorly defined submesothelial layer in *SP*^{-/-} tumors (**B, top**). Masson's trichrome staining revealed increased levels of collagen fibrils in the submesothelial layer as well as within and around the nodular tumors grown in *SP*^{+/+}, relative to *SP*^{-/-} counterparts (**B, middle**). Picosirius red staining showed increased amounts of mature collagen fibers in nodules from *SP*^{+/+} tumors (red under polarized light), compared to less mature fibrils in *SP*^{-/-} tumors (yellow-green under polarized light) (**B, bottom**). Staining results shown are representative of at least three randomly selected areas from serial sections of tumors from five different animals.

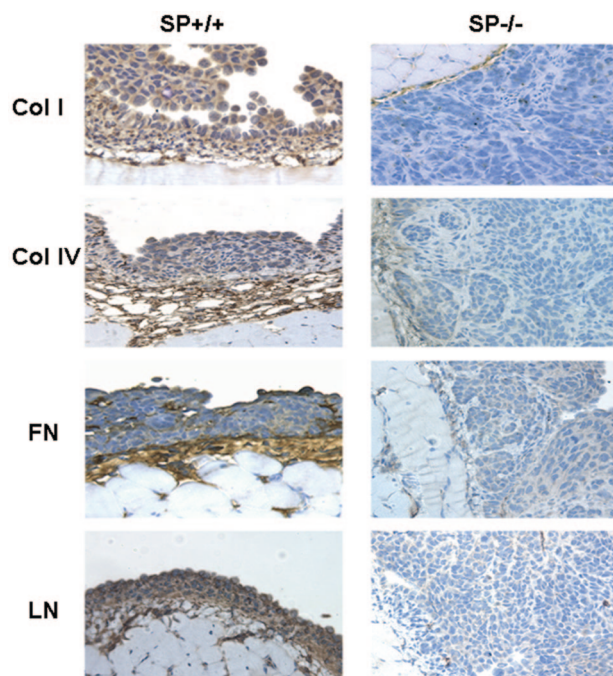


Figure 4. Enhanced growth of peritoneal nodules in $SP^{-/-}$ mice is associated with significantly diminished levels of ECM constituents. Immunohistochemical staining of peritoneal sections revealed defective Col I, Col IV, FN, as well as LN staining within and around the tumor nodules grown in $SP^{-/-}$ as compared to those grown in $SP^{+/+}$ animals. Staining results shown are representative of at least three randomly-selected areas from serial sections of tumors from five different animals.

SPARC Inhibits Proliferation of ID8 Cells *In Vitro* and *In Vivo*

SPARC has been shown to inhibit the proliferation of primary epithelial and mesenchymal cells,³²⁻³⁴ as well as that of primary human ovarian cancer cells and human ovarian cancer cell line SKOV3 *in vitro*.¹⁴ Our finding that tumors grew faster and gave rise to larger nodules in $SP^{-/-}$ mice prompted us to study the effect of SPARC on ID8 cell proliferation *in vitro*. As expected, a pronounced anti-proliferative effect of SPARC was observed at concentrations between 10 to 40 $\mu\text{g/ml}$, as determined by 2-day growth assays (43 to 56% of control) and DNA synthesis assays (75 to 88% of control; Figure 7, A and B). Consistent with these *in vitro* findings, comparison of the peritoneal tumor sections stained for proliferation makers Ki67 (Figure 7, C and D) and phospho-histone 3 (data not shown) revealed a significantly higher (>70%) proliferation index for $SP^{-/-}$ mice, relative to their $SP^{+/+}$ counterparts. Taken together, our results strongly implicate SPARC as a potent inhibitor of ovarian carcinoma cell proliferation *in vitro* and *in vivo*.

SPARC Promotes Apoptosis of ID8 Cells *In Vitro* and *In Vivo*

SPARC has been shown to increase the sensitivity of murine pancreatic cancer cells to the apoptotic effect of anti-cancer agents,²⁶ and to induce apoptosis in human ovarian carcinoma cells *in vitro*.¹³ Herein, we tested the

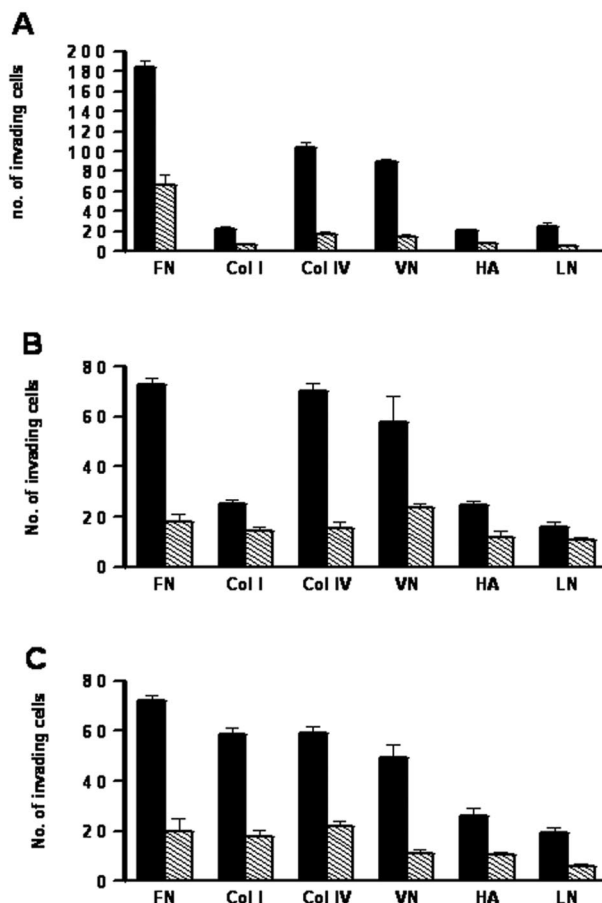


Figure 5. SPARC inhibits the adhesion of ID8 cells to ECM proteins. In solid phase binding assays, ID8 cells (A) readily adhered to various ECM proteins in the presence (hatched bars) or absence (solid bars) of exogenous SPARC (40 $\mu\text{g/ml}$) after 4 hours. Adhesion was significantly inhibited by SPARC for all of the matrices tested ($*P < 0.05$). SPARC also significantly inhibited the adhesion of SKOV3 cells (B), as well as OVCAR3 cells (C) to the same matrices. Bars represent means \pm SEM of a representative experiment that was performed in quadruplicates. The results shown are representative of three independent experiments.

apoptotic effect of SPARC on ID8 cells *in vitro* and *in vivo*. Consistent with previously reported results in human ovarian carcinoma cells, addition of SPARC (40 $\mu\text{g/ml}$) to ID8 cells for 72 hours resulted in a significant (more than threefold) increase in the number of apoptotic cells, as determined by TUNEL assay (Figure 8A) and cleaved caspase-3 staining (data not shown). *In vivo*, peritoneal tumors grown in $SP^{+/+}$ animals were shown to have significantly (approximately threefold) more apoptotic ID8 cells than their $SP^{-/-}$ counterparts, as determined by TUNEL assay (Figure 8B) and cleaved caspase-3 staining (data not shown). Collectively, our results provide strong support for the proapoptotic effects of SPARC on ovarian carcinoma cells *in vitro* and *in vivo*.

Augmented Levels and Activity of VEGF in Ascitic Fluids of $SP^{-/-}$ Mice

High levels of VEGF in malignant ascitic fluid has been correlated with the dissemination of peritoneal carcinomatosis.^{34,35} SPARC has been shown to modulate the

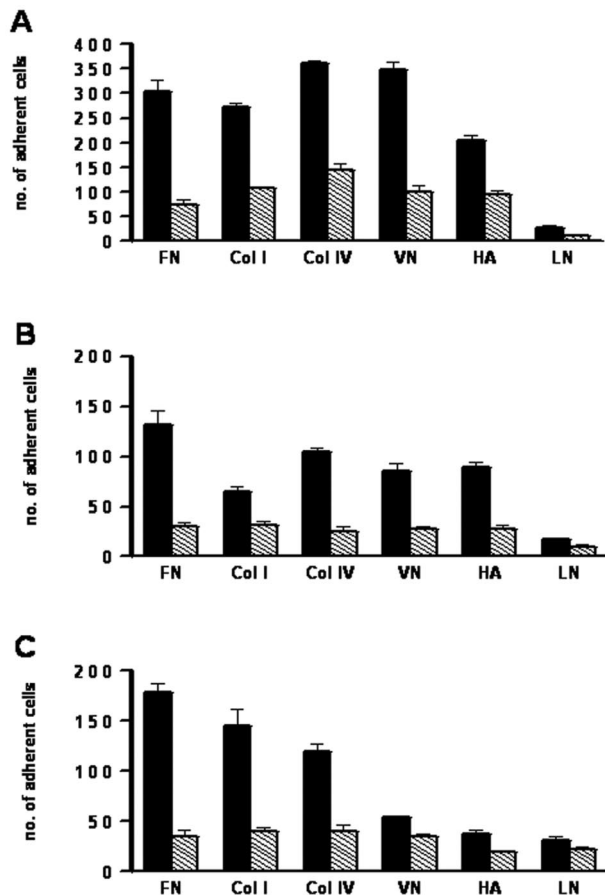


Figure 6. SPARC inhibits invasion of various ECM proteins by ovarian cancer cells. **A:** In a transwell assay, ID8 cells were allowed to invade various ECM-coated inserts in the presence (hatched bars) or absence (solid bars) of exogenous SPARC (40 μ g/ml) for 5 hours. Cell invasion was significantly inhibited by SPARC for all of the matrices tested ($*P < 0.05$). Similarly, SPARC inhibited the invasion of the ECM-coated inserts by OVCAR3 (**B**) and SKOV3 (**C**) human ovarian cancer cell lines. Bars represent the means \pm SEM of a representative experiment that was performed in quadruplicates. The results shown are representative of three independent experiments.

mitogenic activity of VEGF through a direct binding interaction and reduction of the association of VEGF with its cell-surface receptors.³⁶ In the present study, *SP*^{-/-} mice developed more tumor nodules and accumulated larger volumes of hemorrhagic ascitic fluid that contained many floating tumor cells. We therefore hypothesized that in the absence of host SPARC, malignant ascitic fluid with high levels of tumor-derived VEGF would support tumor cell proliferation as well as adhesion to and invasion of peritoneal surfaces, thus promoting further peritoneal involvement and more malignant cell spread. First, we determined the expression levels of VEGF and its receptors VEGFR1, VEGFR2, and neuropilin 1 (Npn 1) in peritoneal tumors from *SP*^{+/+} and *SP*^{-/-} animals. Our results indicated that in the absence of host SPARC, the expression of VEGF, VEGFR2, and Npn 1 were significantly up-regulated in the tumor nodules at the RNA level (Figure 9A), as well as in immunostained tumor sections (Supplemental Figure 3, see <http://ajp.amjpathol.org>). Consistent with these findings, significantly (>2.5-fold) higher levels of VEGF were detected in the ascitic fluid of

SP^{-/-} mice, relative to *SP*^{+/+} counterparts (Figure 9B). To ensure that the increased levels of VEGF in the ascitic fluid of *SP*^{-/-} mice, correlated with increased activity of the growth factor, different dilutions of the ascitic fluid were tested for their growth-promoting activity on ID8 cells *in vitro*. We found that the ascitic fluid collected from *SP*^{-/-} mice induced concentration-dependent proliferation of ID8 cells that was significantly (> twofold) higher than that of *SP*^{+/+} controls (Figure 9C). The proliferative effect of ascitic fluid on ID8 cells was found to be, at least in part, mediated by VEGF, as determined by studies using a VEGF-neutralizing antibody or VEGFR2-specific inhibitors (data not shown). Furthermore, we tested the effect of ascitic fluid on ID8 cell adhesion to and invasion of FN. Whereas both *SP*^{+/+} and *SP*^{-/-} ascitic fluids stimulated ID8 cell adhesion equally (approximately one-fold increase; Figure 9D), *SP*^{-/-} ascitic fluid elicited a more significant increase in invasiveness of ID8 cells plated on FN, relative to *SP*^{+/+} controls (~1.7-fold; Figure 9E). To elucidate the factors implicated in ascitic fluid-augmented invasion of ID8 cells, we determined the RNA expression of MMP-2 and MMP-9 in the peritoneal tumor nodules, as well as their proteolytic activity in gelatin zymograms of ascitic fluid samples collected from *SP*^{+/+} and *SP*^{-/-} tumor-bearing mice. Our results revealed a down-regulated RNA expression of MMP-2 and MMP-9 in tumor nodules from *SP*^{+/+} tumors, relative to *SP*^{-/-} counterparts (data not shown). Moreover, ascitic fluids collected from *SP*^{-/-} animals displayed a pronounced gelatinolytic activity of MMP-2 (72 and 68 kd for the pro and active forms, respectively) and MMP-9 (95 and 105 kd for the pro and active forms, respectively). In sharp contrast, samples from *SP*^{+/+} animals exhibited little or no significant gelatinolytic activity (Figure 9F). Taken together, the observed increased levels and activity of VEGF in the ascitic fluid in combination with an enhanced proteolytic activity could, in part, be responsible for the significantly augmented peritoneal carcinoma-tosis observed in *SP*^{-/-} tumor-bearing mice.

Discussion

The high propensity of epithelial ovarian carcinoma cells to implant onto the peritoneal mesothelial surface of the abdominal cavity, migrate, and invade the submesothelial interstitial (stromal) matrix is believed to play a pivotal role in the metastasis of this deadly disease.⁴ The mesothelial cells lining the peritoneal cavity express various ECM proteins at their cell surface (ie, toward the peritoneal cavity). Thus, offering an anatomical privilege to epithelial ovarian carcinoma to adhere and initiate the cascade of tumor cell colonization, shedding, and recolonization throughout the peritoneal cavity.^{3,37} The contribution of SPARC as an ECM-associated protein in modulating this anatomical privilege has not yet been elucidated. In the present study, we have used *SP*^{-/-} and *SP*^{+/+} mice to study the multifaceted functions of SPARC in the pathogenesis of peritoneal ovarian cancer at different stages of the pathogenic cascade. We have found that absence of SPARC is associated with quanti-

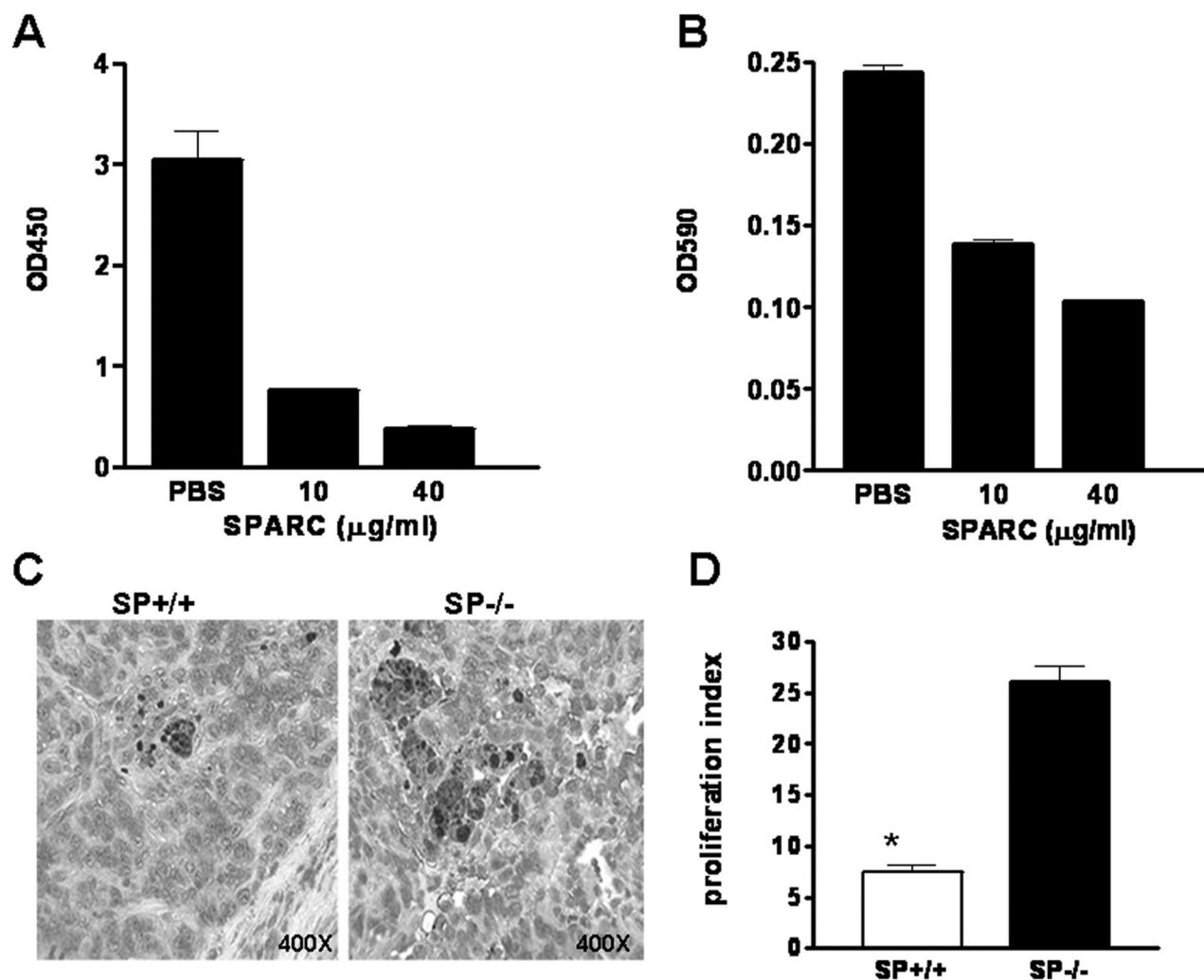


Figure 7. SPARC inhibits the proliferation of ID8 cells *in vitro* and *in vivo*. ID8 cell proliferation in the absence and presence of SPARC (10 to 40 µg/ml) for 48 hours, cell proliferation, and DNA synthesis were measured by MTS production (A) and BrdU incorporation (B), respectively. SPARC significantly inhibited proliferation and DNA synthesis of ID8 cells compared to the PBS control (**P* < 0.05). *In vivo*, immunohistochemical staining of intraperitoneal tumors showed more nuclei stained with Ki67 antibody in tumors grown in SP^{-/-} mice than those in SP^{+/+} mice (**P* < 0.05). The proliferation index of intraperitoneal tumor cells was determined by calculating the mean value of Ki67-positive nuclei per 10 random fields from serial peritoneal sections. C: Bars represent the means ± SEM of cells counted in 10 fields/serial tumor sections from five different animals. The results shown are representative of three independent experiments. Original magnifications, ×400.

tative and qualitative defects of ECM components (particularly Col I) in the normal peritoneum, and that SP^{-/-} peritoneal tumors were associated with significantly diminished levels of BM components (Col IV and LN) and to a lesser extent FN within and around tumor cells. Therefore, it appears that the overall diminution in the levels of ECM components created a permissive environment for the accelerated tumor growth and invasion of ID8 tumor cells in SP^{-/-} mice and may reflect an augmented rate of BM and submesothelial interstitial matrix degradation and/or invasion. Furthermore, the ability of advanced ovarian carcinomas and ascitic fluid spheroids to alter the expression of Col IV and LN has been suggested to reflect the aggressive phenotype that facilitates shedding of cancer cells from primary sites into the peritoneal spaces and their subsequent attachment to the secondary sites.^{38,39}

A number of human ovarian cancer cells lines and cultured ovarian cancer cells recovered from ascites fluid

have been shown to preferentially adhere to Col I,³⁰ as well as to LN, FN, VN, Col IV, and HA.^{2,27,40,41} In the present study, we have shown that similar to OVCAR3 and SKOV3, ID8 cell adhesion to all of the aforementioned matrices was significantly inhibited in the presence of SPARC. To our knowledge, this is the first time that SPARC is shown to exert an anti-adhesive effect on murine and/or human ovarian cancer cell lines. Moreover, we found that similar to human ovarian carcinoma cells (OVCAR3 and SKOV3), ID8 cells significantly invaded FN and the major BM components (Col IV and LN). The adhesion and invasion of ID8 cells, OVCAR3, and SKOV3 cell lines to FN was significant. The synthesis of both ECM-immobilized and soluble FN by mesothelial cells has been shown to be increased in tumor ascites as well as in inflammatory conditions. In either form, FN has been reported to further stimulate ovarian carcinoma cell motility and invasion.^{42,43} Moreover, our findings that ID8, OVCAR3, and SKOV3 cells were also invasive to Col I

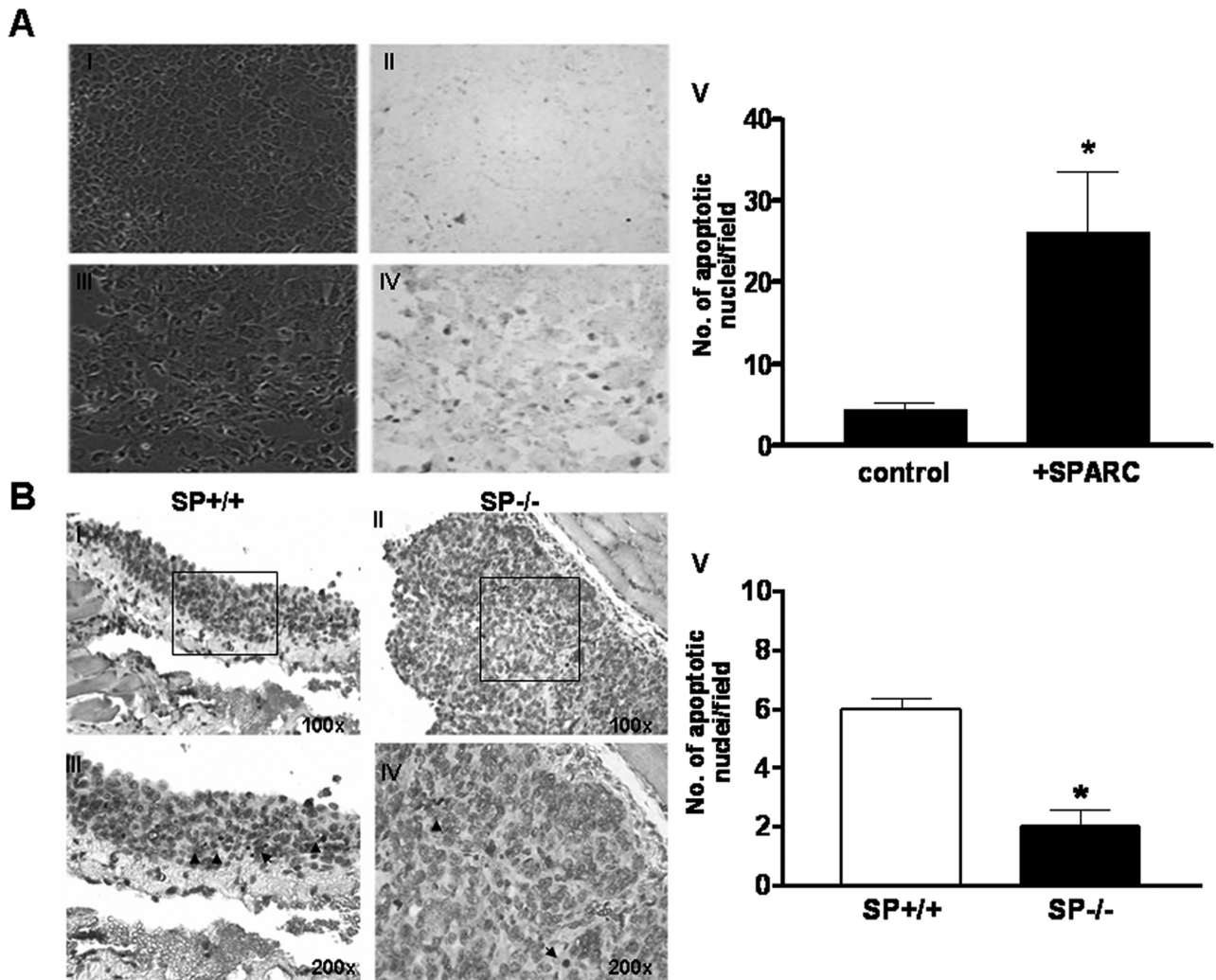


Figure 8. SPARC induces apoptosis in ID8 cells *in vitro* and *in vivo*. *In vitro* TUNEL staining of ID8 cells after a 72-hour incubation with PBS (control; **A, I and II**) and SPARC (40 µg/ml in PBS; **A, III to VI**) revealed that SPARC-treated cells showed more brown-stained small apoptotic nuclei than control cells (**A, II**). The corresponding phase-contrast fields (**A, I and III**) represent the total number of cells in each field. The number of apoptotic nuclei was significantly higher in SPARC-treated cells relative to PBS-treated controls (**A, V**). Bars represent the means \pm SEM of cells counted in 10 fields/experimental condition. Results shown are representative of two independent experiments ($*P < 0.05$). TUNEL staining of peritoneal tumor nodules revealed more apoptotic tumor cells with small apoptotic nuclei and scanty cytoplasm in SP^{+/+} tumors (**B, I and III**), compared to SP^{-/-} tumors (**B, II and IV**). The number of apoptotic nuclei in SP^{+/+} tumors was significantly higher than in SP^{-/-} counterparts (**B, V**). Bars represent the means \pm SEM of cells counted in 10 fields/serial tumor sections from five different animals. The results shown are representative of two independent experiments ($*P < 0.05$).

and VN are in agreement with earlier reports.^{30,40,44} The suppressive effects of SPARC on ovarian cancer cell adhesion to and invasion of BM and ECM components *in vitro* offers a reasonable explanation for our *in vivo* model in which SP^{-/-} mice developed more extensively-disseminated tumors than their SP^{+/+} counterparts.

The adhesion of human ovarian cancer cells to either peritoneal mesothelial cells or submesothelial stromal components has been shown to be mediated through members of the integrin family and several cell surface proteoglycans (heparan sulfate and chondroitin sulfate proteoglycans including syndecans, glypicans, and CD44); all have been shown to be expressed by ovarian carcinoma cells either individually or in combination.^{2,27,37,40,45} These major cell surface receptors have been implicated to mediate the cross-talk between tumor cells and ECM constituents of the host and were shown to be crucial for cell invasion and migration not only for

physically tethering the tumor cells to the matrix but also for sending and receiving molecular signals that regulate the invasive and metastatic processes of malignant cells.^{40,42,46} Our finding that SPARC inhibited both adhesion and invasion of ovarian carcinoma cells to the ECM constituents implies that SPARC could potentially interact with and/or regulate the receptors involved in anchoring the cells to these matrices. These potential interactions are currently under investigation (Said and Motamed, unpublished results).

The level of VEGF expression in tumors and/or ascitic fluid has been directly correlated with increased invasiveness and poor clinical outcome of ovarian cancer.^{36,48} In the present study, we have found that the augmented tumor dissemination in SP^{-/-} mice was not only associated with increased expression of VEGF and VEGFRs in the tumors, but with accumulation of larger volumes of ascitic fluid containing significantly high levels of biolog-

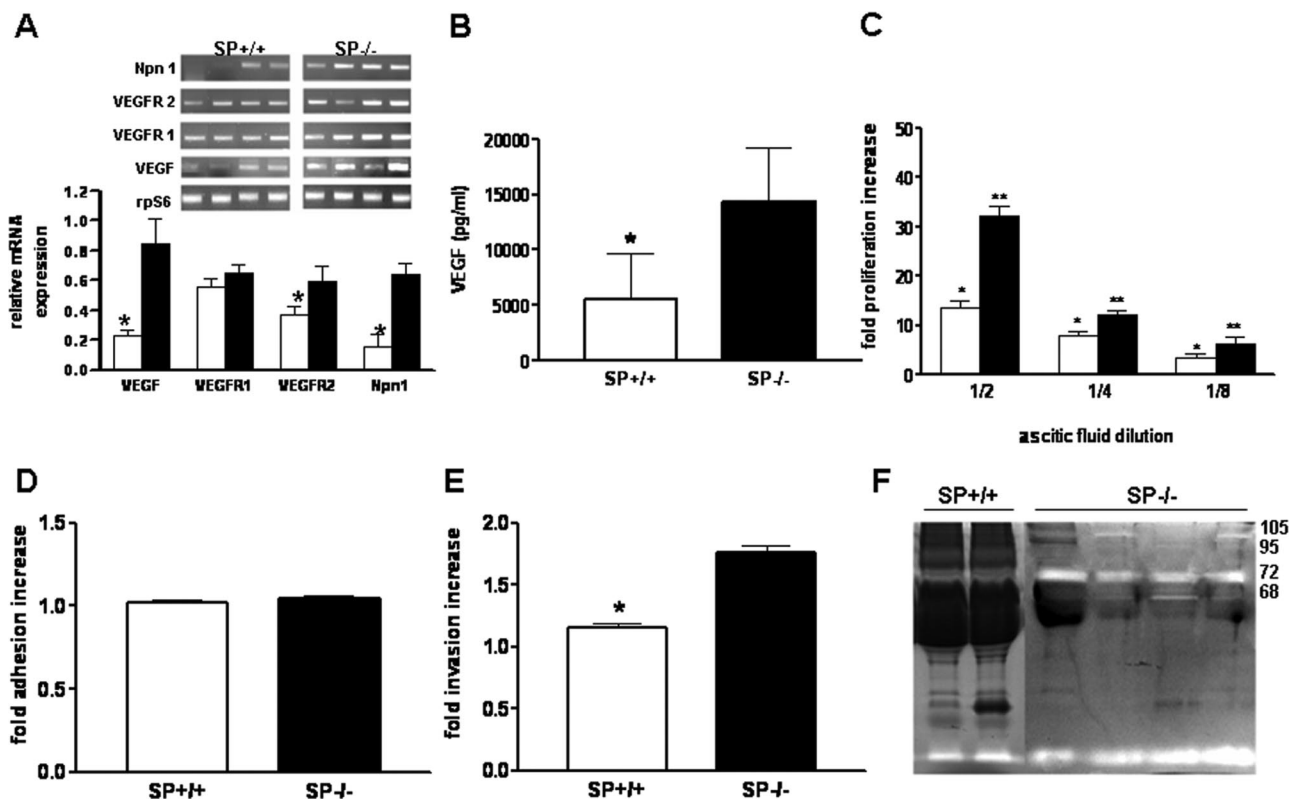


Figure 9. Host SPARC down-regulates the expression and activity of VEGF and gelatinases in ovarian peritoneal carcinomatosis. **A:** Using semiquantitative reverse transcriptase-polymerase chain reaction, significantly higher RNA expression levels of VEGF, VEGFR 2, and Npn 1 were detected in tumor nodules growing in $SP^{-/-}$ animals compared to $SP^{+/+}$ counterparts ($*P < 0.05$). **B:** Ascitic fluid collected from $SP^{-/-}$ mice contained significantly higher levels of VEGF than that of $SP^{+/+}$ mice, as determined by a VEGF ELISA. Bars represent means \pm SEM of a representative experiment that was performed in quadruplicates. The results shown are representative of three independent experiments in three different animals. VEGF activity in pooled ascitic fluids from $SP^{-/-}$ and $SP^{+/+}$ mice ($n = 5$ each) was assessed using proliferation, adhesion, and invasion assay. **C:** Serial dilutions of pooled ascitic fluids of equal total protein content from $SP^{-/-}$ and $SP^{+/+}$ mice were shown to significantly augment DNA synthesis in ID8 cells in a concentration-dependent manner, as determined by an *in vitro* BrdU incorporation assay ($*P < 0.001$ and $*P < 0.05$ for $SP^{-/-}$ and $SP^{+/+}$, respectively). At all tested concentrations, ascitic fluids from $SP^{-/-}$ mice induced significantly higher rates of proliferation than $SP^{+/+}$ ones ($P < 0.05$). Bars represent fold increase proliferation over ID8 cells grown in complete growth medium. Whereas both $SP^{+/+}$ and $SP^{-/-}$ ascitic fluids increased ID8 cell adhesion to FN equally (**D**), $SP^{-/-}$ fluids induced a significantly higher increase in invasion of FN over that of the vehicle-treated controls ($*P > 0.05$) (**E**). Bars represent mean \pm SEM of one experiment performed in triplicates that was representative of three independent experiments. Using gelatin zymography, pooled ascitic fluids from $SP^{-/-}$ mice exhibited significant gelatinolytic activity of pro and active forms of MMP2 (68 and 72 kd) and pro and active forms of MMP-9 (95 and 105 kd), whereas $SP^{+/+}$ ascitic fluids did not show any significant enzymatic activity.

ically active VEGF. Concomitant with the high levels of biologically active VEGF, $SP^{-/-}$ ascitic fluids showed enhanced MMP-2 and MMP-9 proteolytic activities. Increased activity of MMPs has been reported to modulate the bioavailability of VEGF by direct stimulation of VEGF release and mobilization from tumor cells and the ECM resulting in further augmentation of the proliferative, pro-survival, and permeability effects of VEGF.^{48,49} Furthermore, these findings provide supporting evidence that the observed diminution in ECM content in tumor-bearing $SP^{-/-}$ mice was, at least in part, due to increased ECM degradation. Therefore, it can be concluded that ascitic fluid from $SP^{-/-}$ animals is a complex fluid that plays an active role in enhancing ECM degradation, tumor cell proliferation, migration, invasion, and dissemination of tumor cells.

The up-regulation of VEGF has been shown to be a pivotal component of the pathogenesis of epithelial ovarian tumors, in part through increased tumor angiogenesis and/or vasculogenesis.^{35,47,50,51} Our findings revealed that although $SP^{-/-}$ peritoneal tumors displayed more vascular endothelial staining compared to their $SP^{+/+}$

counterparts (data not shown), they exhibited marked heterogeneity not only within the same tumor section but between serial sections from the same tumor, as well as between different animals. Staining pattern was heterogeneous with respect to localization as well as morphology and size of the endothelial-positive areas. On the other hand, we have found significantly increased mean vascular density in $SP^{-/-}$ mice bearing subcutaneous tumors (Supplemental Figure 1, see <http://ajp.amjpathol.org>), compared to the $SP^{+/+}$. Moreover, we and others⁵¹ have found that ID8 cells express VEGF, VEGFR1, and Npn1 but not VEGFR2 (Supplemental Figure 2, see <http://ajp.amjpathol.org>). However, immunostaining of tumors from $SP^{-/-}$ and $SP^{+/+}$ mice revealed increased expression not only of VEGF but VEGFR1 and VEGFR2 $SP^{-/-}$ mice as compared to $SP^{+/+}$ counterparts (Supplemental Figure 3, see <http://ajp.amjpathol.org>). Because SPARC has been shown to abrogate the mitogenic effect of VEGF on endothelial cells *in vitro* and *in vivo*,^{16,36} the increased vascular staining in tumors of $SP^{-/-}$ mice can be attributed, at least in part, to the absence of host SPARC.

In agreement with previously reported anti-proliferative and proapoptotic effects of SPARC on human ovarian cancer cell lines,¹³ addition of exogenous SPARC to murine ID8 cells significantly suppressed their proliferation and augmented their rate of apoptosis. More importantly, we were able to show for the first time that the anti-proliferative and proapoptotic effects of SPARC *in vivo* were more pronounced in peritoneal tumors of *SP*^{+/-} relative to that of *SP*^{-/-} tumors.

In conclusion, we have demonstrated for the first time the role of SPARC as an endogenous negative regulator of ovarian tumor cell adhesion to and invasion of the ECM constituents and the concomitant abrogation of the early events in the cascade of the peritoneal involvement in ovarian cancer. Due to the multifaceted effects of SPARC on inhibition of ovarian carcinoma cell adhesion, invasion, and proliferation, as well as induction of apoptosis, it merits further investigation as a novel endogenous therapeutic candidate in the treatment of ovarian cancer. Moreover, with the advent of recent technologies in genomics research, it remains to be elucidated whether mutations, polymorphisms, deletions, or promoter methylation of the human SPARC gene is associated with susceptibility to pathogenesis and/or progression of ovarian carcinoma.

Acknowledgments

We thank Dr. George Coukos for providing ID8-GFP cells, Dr. E. Helene Sage for providing *SP*^{-/-} and *SP*^{+/-} mice, and Heather Walker and Ida Najwer for technical assistance with immunohistochemistry.

References

- Jemal A, Murray T, Ward E, Samuels A, Tiwari RC, Ghafoor A, Feuer EJ, Thun MJ: Cancer Statistics, 2005. *CA Cancer J Clin* 2005, 55:10–30
- Burleson KM, Casey RC, Skubitz KM, Pambuccian SE, Oegema Jr TR, Skubitz AP: Ovarian carcinoma ascites spheroids adhere to extracellular matrix components and mesothelial cell monolayers. *Gynecol Oncol* 2004, 93:170–181
- Lessan K, Aguiar DJ, Oegema T, Siebenson L, Skubitz AP: CD44 and beta1 integrin mediate ovarian carcinoma cell adhesion to peritoneal mesothelial cells. *Am J Pathol* 1999, 154:1525–1537
- Freedman RS, Deavers M, Liu J, Wang E: Peritoneal inflammation—a microenvironment for epithelial ovarian cancer (EOC). *J Transl Med* 2004, 2:23
- Akutagawa N, Nishikawa A, Iwasaki M, Fujimoto T, Teramoto M, Kitajima Y, Endo T, Shibuya M, Kudo R: Expression of vascular endothelial growth factor and E-cadherin in human ovarian cancer: association with ascites fluid accumulation and peritoneal dissemination in mouse ascites model. *Jpn J Cancer Res* 2002, 93:644–651
- Brekken RA, Sage EH: SPARC, a matricellular protein: at the crossroads of cell-matrix communication. *Matrix Biol* 2001, 19:816–827
- Bradshaw AD, Sage EH: SPARC, a matricellular protein that functions in cellular differentiation and tissue response to injury. *J Clin Invest* 2001, 107:1049–1054
- Framson PE, Sage EH: SPARC and tumor growth: where the seed meets the soil? *J Cell Biochem* 2004, 92:679–690
- Brekken RA, Puolakkainen P, Graves DC, Workman G, Lubkin SR, Sage EH: Enhanced growth of tumors in SPARC null mice is associated with changes in the ECM. *J Clin Invest* 2003, 111:487–495
- Ledda MF, Adris S, Bravo AI, Kairiyama C, Bover L, Chernajovsky Y, Mordoh J, Podhajcer OL: Suppression of SPARC expression by antisense RNA abrogates the tumorigenicity of human melanoma cells. *Nat Med* 1997, 3:171–176
- Schultz C, Lemke N, Ge S, Golembieski WA, Rempel SA: Secreted protein acidic and rich in cysteine promotes glioma invasion and delays tumor growth in vivo. *Cancer Res* 2002, 62:6270–6277
- Mok SC, Chan WY, Wong KK, Muto MG, Berkowitz RS: SPARC, an extracellular matrix protein with tumor-suppressing activity in human ovarian epithelial cells. *Oncogene* 1996, 12:1895–1901
- Yiu GK, Chan WY, Ng SW, Chan PS, Cheung KK, Berkowitz RS, Mok SC: SPARC (secreted protein acidic and rich in cysteine) induces apoptosis in ovarian cancer cells. *Am J Pathol* 2001, 159:609–622
- Delany AM, Kalajic I, Bradshaw AD, Sage EH, Canalis E: Osteonectin-null mutation compromises osteoblast formation, maturation, and survival. *Endocrinology* 2003, 144:2588–2596
- Francki A, Bradshaw AD, Bassuk JA, Howe CC, Couser WG, Sage EH: SPARC regulates the expression of collagen type I and transforming growth factor-beta1 in mesangial cells. *J Biol Chem* 1999, 274:32145–32152
- Bradshaw AD, Reed MJ, Carbon JG, Pinney E, Brekken RA, Sage EH: Increased fibrovascular invasion of subcutaneous polyvinyl alcohol sponges in SPARC-null mice. *Wound Repair Regen* 2001, 9:522–530
- Bradshaw AD, Reed MJ, Sage EH: SPARC-null mice exhibit accelerated cutaneous wound closure. *J Histochem Cytochem* 2002, 50:1–10
- Puolakkainen P, Bradshaw AD, Kyriakides TR, Reed M, Brekken R, Wight T, Bornstein P, Ratner B, Sage EH: Compromised production of extracellular matrix in mice lacking secreted protein, acidic and rich in cysteine (SPARC) leads to a reduced foreign body reaction to implanted biomaterials. *Am J Pathol* 2003, 162:627–635
- Bradshaw AD, Puolakkainen P, Dasgupta J, Davidson JM, Wight TN, Helene Sage E: SPARC-null mice display abnormalities in the dermis characterized by decreased collagen fibril diameter and reduced tensile strength. *J Invest Dermatol* 2003, 120:949–955
- Bassuk JA, Birkebak T, Rothmier JD, Clark JM, Bradshaw A, Muchowski PJ, Howe CC, Clark JI, Sage EH: Disruption of the Sparc locus in mice alters the differentiation of lenticular epithelial cells and leads to cataract formation. *Exp Eye Res* 1999, 68:321–331
- Gilmour DT, Lyon GJ, Carlton MB, Sanes JR, Cunningham JM, Anderson JR, Hogan BL, Evans MJ, Colledge WH: Mice deficient for the secreted glycoprotein SPARC/osteonectin/BM40 develop normally but show severe age-onset cataract formation and disruption of the lens. *EMBO J* 1998, 17:1860–1870
- Yan Q, Blake D, Clark JI, Sage EH: Expression of the matricellular protein SPARC in murine lens: SPARC is necessary for the structural integrity of the capsular basement membrane. *J Histochem Cytochem* 2003, 51:503–511
- Roby KF, Taylor CC, Sweetwood JP, Cheng Y, Pace JL, Tawfik O, Persons DL, Smith PG, Terranova PF: Development of a syngeneic mouse model for events related to ovarian cancer. *Carcinogenesis* 2000, 21:585–591
- Zhang L, Yang N, Garcia JR, Mohamed A, Benencia F, Rubin SC, Allman D, Coukos G: Generation of a syngeneic mouse model to study the effects of vascular endothelial growth factor in ovarian carcinoma. *Am J Pathol* 2002, 161:2295–2309
- Shibata K, Kikkawa F, Nawa A, Tamakoshi K, Suganuma N, Tomoda Y: Increased matrix metalloproteinase-9 activity in human ovarian cancer cells cultured with conditioned medium from human peritoneal tissue. *Clin Exp Metastasis* 1997, 15:612–619
- Puolakkainen PA, Brekken RA, Muneer S, Sage EH: Enhanced growth of pancreatic tumors in SPARC-null mice is associated with decreased deposition of extracellular matrix and reduced tumor cell apoptosis. *Mol Cancer Res* 2004, 2:215–224
- Buczek-Thomas JA, Chen N, Hasan T: Integrin-mediated adhesion and signaling in ovarian cancer cells. *Cell Signal* 1998, 10:55–63
- Sage H, Vernon RB, Funk SE, Everitt EA, Angello J: SPARC, a secreted protein associated with cellular proliferation, inhibits cell spreading in vitro and exhibits Ca²⁺-dependent binding to the extracellular matrix. *J Cell Biol* 1989, 109:341–356
- Motamed K, Sage EH: SPARC inhibits endothelial cell adhesion but not proliferation through a tyrosine phosphorylation-dependent pathway. *J Cell Biochem* 1998, 70:543–552
- Kokenyesi R, Murray KP, Benschushan A, Huntley ED, Kao MS: Invasion of interstitial matrix by a novel cell line from primary peritoneal

- carcinosarcoma, and by established ovarian carcinoma cell lines: role of cell-matrix adhesion molecules, proteinases, and E-cadherin expression. *Gynecol Oncol* 2003, 89:60–72
31. Schiemann BJ, Neil JR, Schiemann WP: SPARC inhibits epithelial cell proliferation in part through stimulation of the transforming growth factor-beta-signaling system. *Mol Biol Cell* 2003, 14:3977–3988
 32. Funk SE, Sage EH: Differential effects of SPARC and cationic SPARC peptides on DNA synthesis by endothelial cells and fibroblasts. *J Cell Physiol* 1993, 154:53–63
 33. Motamed K, Funk SE, Koyama H, Ross R, Raines EW, Sage EH: Inhibition of PDGF-stimulated and matrix-mediated proliferation of human vascular smooth muscle cells by SPARC is independent of changes in cell shape or cyclin-dependent kinase inhibitors. *J Cell Biochem* 2002, 84:759–771
 34. Mesiano S, Ferrara N, Jaffe RB: Role of vascular endothelial growth factor in ovarian cancer: inhibition of ascites formation by immunoneutralization. *Am J Pathol* 1998, 153:1249–1256
 35. Yabushita H, Shimazu M, Noguchi M, Kishida T, Narumiya H, Sawaguchi K: Vascular endothelial growth factor activating matrix metalloproteinase in ascitic fluid during peritoneal dissemination of ovarian cancer. *Oncol Rep* 2003, 10:89–95
 36. Kupprion C, Motamed K, Sage EH: SPARC (BM-40, osteonectin) inhibits the mitogenic effect of vascular endothelial growth factor on microvascular endothelial cells. *J Biol Chem* 1998, 273:29635–29640
 37. Strobel T, Cannistra SA: Beta1-integrins partly mediate binding of ovarian cancer cells to peritoneal mesothelium in vitro. *Gynecol Oncol* 1999, 73:362–367
 38. Yang DH, Smith ER, Cohen C, Wu H, Patriotic C, Godwin AK, Hamilton TC, Xu XX: Molecular events associated with dysplastic morphologic transformation and initiation of ovarian tumorigenicity. *Cancer* 2002, 94:2380–2392
 39. Capo-Chichi CD, Smith ER, Yang DH, Roland IH, Vanderveer L, Cohen C, Hamilton TC, Godwin AK, Xu XX: Dynamic alterations of the extracellular environment of ovarian surface epithelial cells in pre-malignant transformation, tumorigenicity, and metastasis. *Cancer* 2002, 95:1802–1815
 40. Cannistra SA, Ottensmeier C, Niloff J, Orta B, DiCarlo J: Expression and function of beta 1 and alpha v beta 3 integrins in ovarian cancer. *Gynecol Oncol* 1995, 58:216–225
 41. Cannistra SA, Abu-Jawdeh G, Niloff J, Strobel T, Swanson L, Andersen J, Ottensmeier C: CD44 variant expression is a common feature of epithelial ovarian cancer: lack of association with standard prognostic factors. *J Clin Oncol* 1995, 13:1912–1921
 42. Rieppi M, Vergani V, Gatto C, Zanetta G, Allavena P, Taraboletti G, Giavazzi R: Mesothelial cells induce the motility of human ovarian carcinoma cells. *Int J Cancer* 1999, 80:303–307
 43. Gerbes AL, Jungst D, Xie YN, Permanetter W, Paumgartner G: Ascitic fluid analysis for the differentiation of malignancy-related and nonmalignant ascites. Proposal of a diagnostic sequence. *Cancer* 1991, 68:1808–1814
 44. Beck V, Herold H, Bengel A, Lubert B, Hutzler P, Tschesche H, Kessler H, Schmitt M, Geppert H-G, Reuning U: ADAM15 decreases integrin [alpha]v[beta]3/vitronectin-mediated ovarian cancer cell adhesion and motility in an RGD-dependent fashion. *Int J Biochem Cell Biol* 2005, 37:590–603
 45. Kokenyesi R: Ovarian carcinoma cells synthesize both chondroitin sulfate and heparan sulfate cell surface proteoglycans that mediate cell adhesion to interstitial matrix. *J Cell Biochem* 2001, 83:259–270
 46. Graves LE, Ariztia EV, Navari JR, Matzel HJ, Stack MS, Fishman DA: Proinvasive properties of ovarian cancer ascites-derived membrane vesicles. *Cancer Res* 2004, 64:7045–7049
 47. Bamberger ES, Perrett CW: Angiogenesis in epithelial ovarian cancer. *Mol Pathol* 2002, 55:348–359
 48. Davidson B: Ovarian carcinoma and serous effusions. Changing views regarding tumor progression and review of current literature. *Anal Cell Pathol* 2001, 23:107–128
 49. Belotti D, Paganoni P, Manenti L, Garofalo A, Marchini S, Taraboletti G, Giavazzi R: Matrix metalloproteinases (MMP9 and MMP2) induce the release of vascular endothelial growth factor (VEGF) by ovarian carcinoma cells: implications for ascites formation. *Cancer Res* 2003, 63:5224–5229
 50. Hu L, Hofmann J, Zaloudek C, Ferrara N, Hamilton T, Jaffe RB: Vascular endothelial growth factor immunoneutralization plus Paclitaxel markedly reduces tumor burden and ascites in athymic mouse model of ovarian cancer. *Am J Pathol* 2002, 161:1917–1924
 51. Zhang L, Yang N, Park JW, Katsaros D, Fracchioli S, Cao G, O'Brien-Jenkins A, Randall TC, Rubin SC, Coukos G: Tumor-derived vascular endothelial growth factor up-regulates angiopoietin-2 in host endothelium and destabilizes host vasculature, supporting angiogenesis in ovarian cancer. *Cancer Res* 2003, 63:3403–3412